A Study on Pool Flame Structure Using Thermography

HIROSHI HAYASAKA
Faculty of Engineering
Hokkaido University, Sapporo, Japan

ABSTRACT

Pool flames of heptane, kerosene, and crude oil in a 2.7m square tank were measured by thermography, storing thermal images as TV color images with 25,600 data points every 0.1 second. These apparent temperature images can be converted to irradiance by simple approximations. A series of data recorded continuously at 0.1 second intervals (70 images for one fuel) were analyzed statistically to obtain the distribution of mean radiance, standard deviation and coefficient of variation in the thermography image. The contours of mean radiance, standard deviation and coefficient of variation related to radiance were made, and the flame structure of pool flames are considered from a radiation point of view. The height of maximum radiance from the tank top are obtained from the contours of the mean radiance. Mean paths of formation, growth, and dissipation of vortices are obtained by the contours of the standard deviation on radiance. The stable flame regions and the lower part of plume regions are also obtained by using the contours of the coefficient of variation based on radiance. Flame structures obtained by processing thermographic data are also compared with previous work by McCaffrey who defined flame, intermittent, and plume regions by the temperature and velocity distribution along the center line of flames. By this comparison, statistical analysis using thermographic data is also useful to assess the flame structure of large pool fire flames. Finally, the radiative characteristics of the continuous flame, intermittent, and plume regions, are established.

KEYWORDS: Pool flame, Flame structure, Fire, Thermography, Radiance, Irradiance

INTRODUCTION

In fire fighting and fire safety science, the estimation of thermal radiation from tank fires to the surroundings is important. Many experimental and theoretical studies have been performed on this. Thomas [1], Akita and Yumoto [2], Yumoto [3], McCaffrey [4], and Cetegen et al. [5] have contributed experimental studies on the flame structure, local irradiance and local temperature of large diffusion flames. Koseki and Yumoto [6] measured the irradiance distribution of large heptane flames by a narrow angle thermopile-type radiometer. Ndubizu et al. [7], Crocker and Napier [8], Mudan [9], and Hayasaka and Koseki [10] reported theoretical studies on modeling pool fires.

Recently new techniques have been developed and used in fire experiments. Brötz et al. [11] have developed the equidensitometry technique based on the sensitometric wedge method. By processing a photographic negative using electronic equidensitometry, they determined life-times and migration velocities of eddies, etc. in the pool flames. Oka and Sugawa [12] obtained flame temperature distributions by thermography. These new techniques are very effective in obtaining both instantaneous and mean characteristics of flames but there are difficulties with extracting statistical data such as standard deviation and coefficient of variation of radiance which would help establish the flame structure of pool flames.

To overcome this, an alternative use of thermography has been developed by the author. Here, thermography is used to obtain the irradiance distribution rather than the temperature distribution in pool flames of various fuels. Commercial thermography measures the apparent temperature distribution which may then be converted to irradiance. Little is known, however, of the effect of the combined radiation and combustion phenomena in pool flames. In a large pool flame, radiation may control the burning rate and affect the combustion conditions in the flame. More information of radiation in pool flames may lead to the development of better ways to control this kind of fire. From this point of view, conversion from temperature to irradiance may be useful.

Experiments were conducted to determine the radiation characteristics of pool fires. The apparent temperature data obtained by thermography were converted to irradiance and radiance by simple calculations. Finally, statistical analysis related to radiance data was made to obtain the mean radiance and flame structure of the pool fire flames of the three different fuels.

EXPERIMENT

Pool fire tests were conducted in a quiescent atmosphere in a large indoor test space at the FRI (Fire Research Institute of Japan, test room 24m wide, 24m deep and 20m high). A 2.7m square tank was used for the pool fire tests. The burning rate was measured by an electric float level

meter. Heptane, kerosene, and crude oil were used as test fuels. Each fuel was fed on water to create a 0.02-0.03 m thick layer and then finally make 0.03 m freeboard before the test. The apparent temperature distribution of the pool flame was obtained with color television thermography which stored whole images of the pool flame on a floppy disk at a maximum speed of 20 frames/sec.. The thermographic equipment was installed at 7.93D (D is a the tank diameter, 2.7m in this paper) and the apparent temperature distributions were converted to radiance distributions and irradiance using simple calculations. The irradiance of the pool flames was also measured with a conventional thermopile type radiometer installed at 7D, and the radiometer and thermography data were compared to verify the validity of the thermographic data.

THERMOGRAPHY

The specifications of the thermography used in the experiment are shown in Table 1. The high response detector InSb is cooled by argon gas, and provides whole pool flame images instantaneously. The data of the images can be stored at 0.05 second intervals or slower (0.5, 1 or several seconds). The digital data may be reused and converted to physical quantities like temperature, irradiance, etc..

TABLE 1 Thermography specifications

Type	TVS-3000 (Nippon Avionics Co.,LTD)
Detector	InSb (Indium-Antimony)
Detector coolant	Argon gas
Spectral range	3.0 to 5.4 microns
Scanning method	Rotating mirror wheel
Focus range	254mm to infinity
Field of view	15° horizontal x 10° vertical
Accuracy	±0.4% range (full scale)
Frame time	0.05 sec.
Emissivity compensation	1.00 to 0.10 0.01 step
Spatial resolution	2.18 mrad (0.128°)
Display	10-inch RGB color monitor
Display levels	16 colors
Display resolution (interpolation)	200 lines vertical (100x256=25,600 dots)
Time constant	< 1μsec.

A thermograph is a radiation thermometer. The detector is a radiometer, and the output is interpreted in terms of temperature, considering the distance to the object, emissivity, and the area of the object, defined by the field of view or thermographic specifications. This conversion is simple and reliable when the object is a solid with known emissivity and area. When the object is gaseous, like pool flames, the distance to the object, emissivity, and area of object cannot easily be defined. As a result, direct thermographic images cannot be used as they indicate incorrect or apparent temperature distributions.

In this paper, an imaginary wall of black body specifications is introduced in front of pool flames and conversion of the apparent temperature distribution into radiance distribution is made to determine the thermal structure of the large scale pool flames. Initially it is assumed that the imaginary wall is at the edge of the tank as indicated in Figure 1. A data point, s, does not always represent the radiance of a pool flame just behind the imaginary wall, however, when the distance L is relatively large, as in this experiment, we may assume that the measured, apparent

temperature distribution at the center of a thermographic image will not contain large location errors.

The apparent temperature distribution can be converted to a radiance distribution by the calculations below. Thermography converts radiation heat to apparent temperature, T_a (K), with Equation (1):

$$T_a=(q_s(i,j)/(\varepsilon_s\sigma a_t))^{0.25} \quad (1)$$

where $q_s(i,j)$ is the radiance of data point s on the imaginary wall (kW/m^2), i,j is an index of the horizontal (x-axis) and vertical (z-axis) location and takes values of 1 to 100 and 1 to 256, ε_s is the emissivity of data point s (=1), σ is the Stefan-Boltzmann constant (5.67x10^{-8} W/m^2/K^4); a_t is the area of a data point (m^2) obtained by the equation for TVS-3000. Here L is the measured distance between thermography and imaginary wall (m) and the constants are coefficients in a simple equation related to the view angle of the thermography.

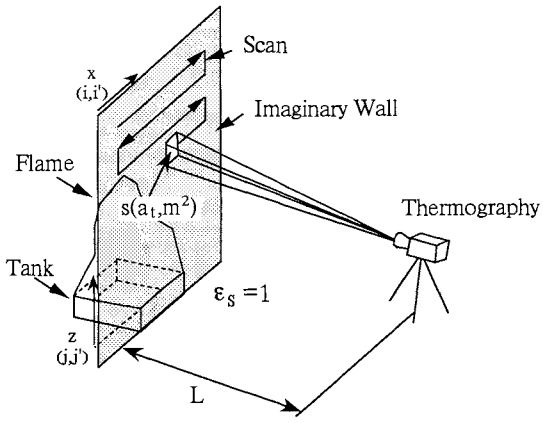

FIGURE 1 Thermography measurements

Thus the radiance of s can be determined with $q_s(i,j)=\sigma\, a_t\, T_a^4$ derived from Equation (1): The total radiation heat from an imaginary wall can be obtained with Equation (2).

$$Q_s=\sum_{i=1}^{m}\sum_{j=1}^{n} q_s(i,j) \quad (2)$$

where m=100 and n=256. Finally, Q_s which is the irradiance observed at the distance L, is converted at the dimensionless distance of L/D=5 to compare it with the data of a wide angle radiometer and it has the unit kW/m^2; $q_s(i,j)$ is simply divided by a solid angle(2π) for a hemisphere of one side of the imaginary wall to convert it to radiance, to show how much radiative heat is emitted from the flame surface within a unit area to the surroundings per unit solid angle, $q_s(i,j)$ has the unit kW/m^2/sr.

Seventy continuous thermographic images are stored and processed by a personal computer to obtain the distribution of mean radiance, standard deviation and coefficient of variation. In this process, a 4x4 matrix of sixteen contiguous data points are integrated into one new data point. Thus, 25,600 (=100x256) data points are reduced to 1,600 (=25x64) to provide a smoother contour. Now, $q_{s,k}(i',j')$ is introduced to represent the radiance of each new data point. The suffix k is the thermographic image number 1 to 70, i',j' is the location of a thermographic image and takes values of 1 to 25 and 1 to 64.

RESULTS AND DISCUSSION

Irradiance of Three Different Fuels

The irradiance of the three fuels are shown in Figure 2. The abscissa is the picture number and the 70 pictures are taken at 0.1 second intervals under the steady state condition. The ordinate is the irradiance at the dimensionless distance L/D=5. The irradiance of heptane, kerosene, and crude oil are shown by crosses, open circles, and solid diamonds respectively. Three horizontal dashed lines show the mean values of the seventy data sets of the three fuels. Figure 2 shows that the mean irradiance of heptane is the highest and that of crude oil is the lowest. Each symbol in Figure 2 is the result of a thermographic image which contains 25,600 data points. These data are processed by a personal computer to create the contour of mean radiance, standard deviation, and coefficient of variation. Since some of these contours and verification ot this technique have already been reported by Hayasaka, Koseki and Tashiro [13,14], only contours for kerosene are shown in Figures 3,4 and 5. Figures 3 shows the mean radiance per unit area and unit solid angle; $\bar{q}_s(i',j')/2\pi$, kW/m²/sr. The thermographic images of pool fire flames show a varied and complex radiance distribution, while the contours of the mean radiance have a smooth parabolic shape. The center of the high radiance zone (above 24 kW/m²/sr) center shown in Figure 3 is at about 0.2D from the tank top.

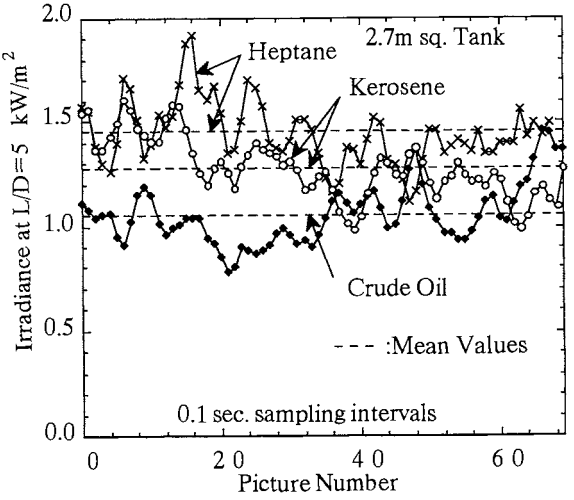

FIGURE 2 Irradiance of the three fuels

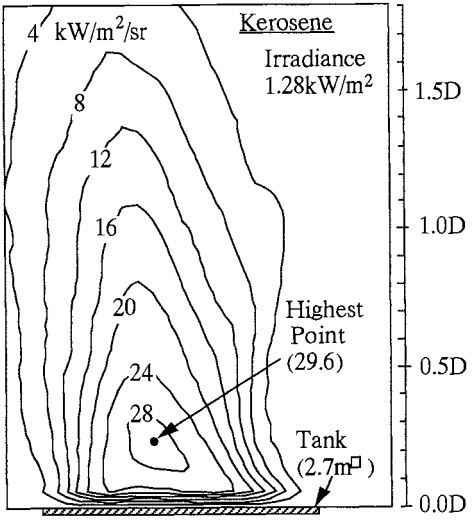

FIGURE 3 Radiance of Kerosene flame

Hägglund [15] reported the average value of the flame radiance from aviation fuel pool fires with a mean radiance value of 8 kW/m^2/sr for a 3 meter square tank. And the contour of radiance for 2 meter fire obtained by the thermovision (AGA 750) is also similar in shape and value to the contours in Figure 3.

The contours of standard deviation in Figure 4 indicate that all the flames have bigger values at the edge than in the center of the flames. Where the standard deviation is large, both the mean value and fluctuations are relatively large. The highest values of the standard deviation at some height over the tank are connected by dashed lines in Figure 4 and the two dashed lines are nearly symmetric and are considered to represent the average vortex paths where vortices are formed, grow, and dissipate. Vortices are also observed near the edge of the flames on the continuous pictures of ordinary video film (30 frames per second, shutter speed 1/4000). But further study is needed to determine the relationship among the high values of standard deviation, vortices, and fluctuation of flames.

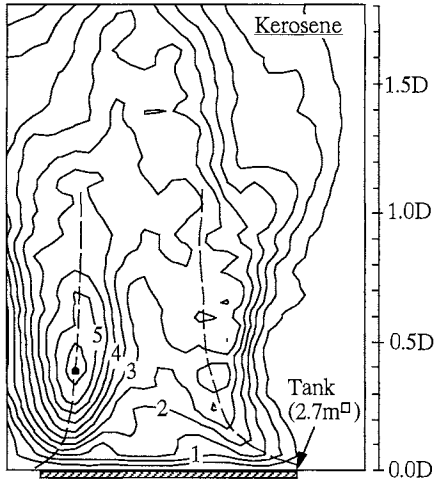

FIGURE 4 Standard deviation of Kerosene flame

The contour of coefficient of variation in Figure 5 shows that the kerosene flame has a region of smaller values at the center of the flame. The coefficient of variation expresses the magnitude of relative fluctuations irrespective of the magnitude of the mean value. The triangular regions at the center of the flame, where the coefficient of variation is below 30%, are stable, continuous flame regions. The high (over 150%) coefficient of variation in the lower part of the plume region shows where large vortices are formed. The edge of horizontally spread out flames (possibly mushroom shaped) sometimes appears in the region of high (over 150%) coefficients of variation in Figure 5.

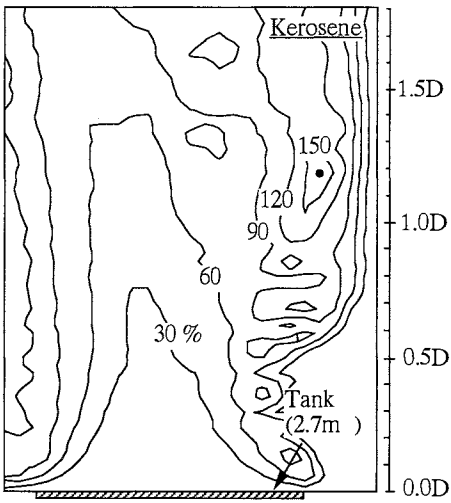

FIGURE 5 Coef. of variation of Kerosene flame

Bouhafid et al. [16] reported the fluctuating character at the base of a pool flame. They concluded that the flame at the pool fire base is better described as a fluctuating, laminar, diffusion

flame, which later becomes a turbulent, intermittent one as it evolves upward along the fire plume. Results for standard deviation and coefficient of variation support these conclusions. The persistent flame has low values of coefficient of variation and regions near the edge of the persistent flame have high values of standard deviation.

Comparison with McCaffrey's Results

Thomas [1] and McCaffrey [4] studied the flame structure of buoyant diffusion flames like pool fire flames. The upward radiance distribution at the flame center, according to their ideas, is shown in Figure 6. The flame center axes are defined as vertical lines perpendicular to the tank. A theoretical expression to characterize buoyant diffusion flames, $z/Q_c^{2/5}$, is used in the abscissa of Figure 6; where z is the vertical height from the tank top, Q_c is the nominal rate of heat release by combustion (kW) which can be obtained from Table 2.

McCaffrey defined three distinct regions, a continuous flame region where temperatures rise above ambient temperatures, (K), and where ΔT is constant; an intermittent region where ΔT is falling with the first power of z; and a plume region where ΔT is falling with the -5/3 power of z. The boundary of these three regions coincides with the intersections of two of the three lines. The intersection of $(z/Q_c^{2/5})^0$ and $(z/Q_c^{2/5})^{-1}$ is the boundary between the continuous flame region and the intermittent region. The intersection of $(z/Q_c^{2/5})^{-1}$ and $(z/Q_c^{2/5})^{-5/3}$ is the boundary between the intermittent and the plume region.

TABLE 2 Burning rate and heat of combustion

	Heptane	Kerosene	Crude oil
Burning rate ($g/m^2/sec.$)	81.4	39.5	38.3
Heat of combustion (MJ/kg)	41.3	41.1	41.9*

* : Estimated value

The boundary values in Figure 6 are smaller than the published values of 0.08 and 0.2. The difference is probably due to the scale of the pool fire and a stronger soot effect. McCaffrey used a small 0.3 m square natural gas burner in a porous refractory material. His flames were more stable, homogeneous, and sootless than the 2.7

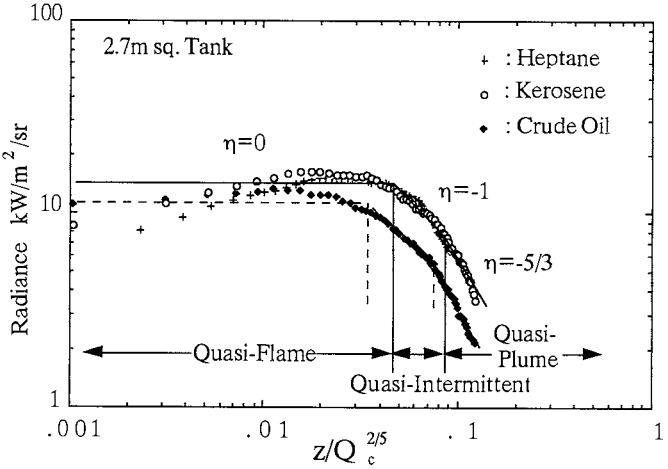

FIGURE 6 Radiance distribution at flame center

m tank flames here, which give off soot, intense radiation, and are heterogeneous due to the liquid fuels. Hence a prefix, quasi-, is used here to distinguish the three regions in Figure 6 from the original three regions.

In Figure 6, the height of the quasi-flame and quasi-intermittent intersection, $z/Q_c^{2/5}$, is 0.045 for heptane and kerosene, and 0.035 for crude oil. The quasi-intermittent and quasi-plume intersection, $z/Q_c^{2/5}$, is 0.085 for heptane and kerosene, and 0.075 for crude oil.

The smaller value for crude oil may be due to severe soot formation. This implies that crude oil has a lower combustion efficiency and larger radiation loss than the other fuels. Lower combustion efficiency, around 80% (Koseki and Mulholland [17]), decreases the value of Q_c in Table 2 assuming complete combustion. In addition, the larger radiation loss of crude oil decreases flame temperature more rapidly than the other fuels. This may lead to a shortening of the flame region height.

Total Structure of Three Flames

The total structure of the flames of the three different fuels are shown in Figures 7, 8, and 9 using the contours of the coefficients of variation. The contours of the coefficient of variation in Figures 7, 8, and 9 , give a height of $z/Q_c^{2/5}$ of 0.045, around a 20-30% coefficient of variation, 23% for heptane, 26% for kerosene, and 20% for crude oil. The height of $z/Q_c^{2/5}$, 0.085, corresponds to a nearly 150% coefficient of variation for all the fuels. The location of the closed square in Figures 7, 8, and 9 show the highest value of radiance in each Figure. Thick dashed lines are the average vortex paths obtained from the contours of the standard deviation and the open triangle indicates the largest value of standard deviation in Figures 7, 8, and 9.

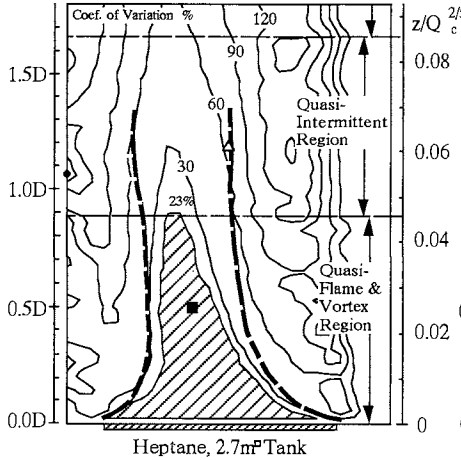

FIGURE 7 Flame structure of Heptane flame

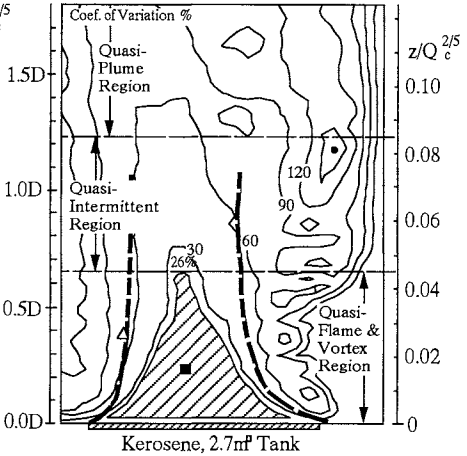

FIGURE 8 Flame structure of Kerosene flame

Flame heights at the upper limit of the quasi-flame regions of each flame are about 0.9D from the tank top for heptane, 0.65D for kerosene, and 0.5D for crude oil. The values of the coefficient of variation at each location are about 23% for heptane, 26% for kerosene, and 20% for crude oil. The boundaries in the radial (horizontal, x-axis) direction of the each stable or persistent flame region are defined by the above mentioned values of the coefficient of variation. The quasi-flame regions are shown by hatching in Figures 7, 8, and 9.

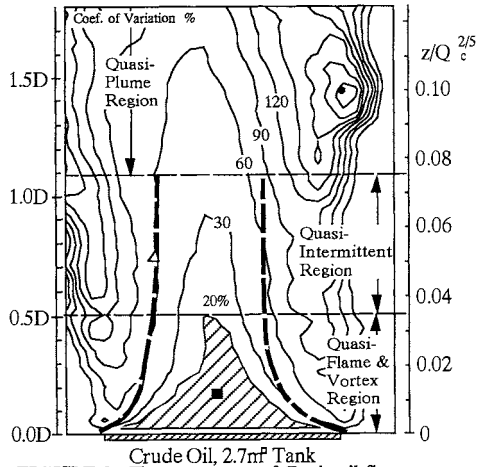

FIGURE 9 Flame structure of Crude oil flame

Irradiance characteristics of each region

Irradiance of the quasi-flame, quasi-intermittent, and quasi-plume region are extracted from thermographic data with the boundary values of $z/Q_c^{2/5}$ for each region. Figures 10, 11, and 12 are for the three fuels, heptane in Figure 10, kerosene in Figure 11, and crude oil in Figure 12. The figures show irradiances of the total, quasi-flame and vortex, quasi-intermittent and quasi-plume regions. Here the quasi-flame and vortex regions are used to distinguish the stable or persistent flame region. Total irradiances are the same as in Figure 2. The dotted lines in each figure are mean values of irradiance. The irradiance of the quasi-plume region of heptane in Figure 10 were smaller than the other two flames because the heptane flame height was taller and the top of the flame was outside the range of the thermogra-

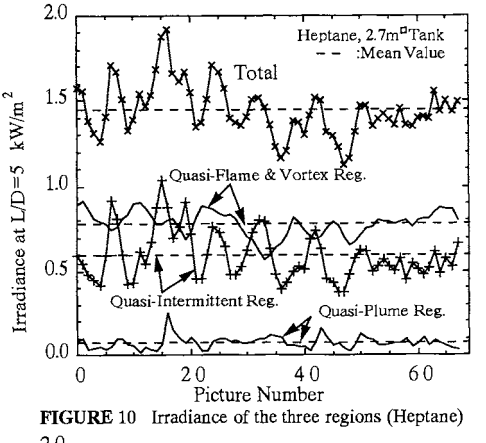

FIGURE 10 Irradiance of the three regions (Heptane)

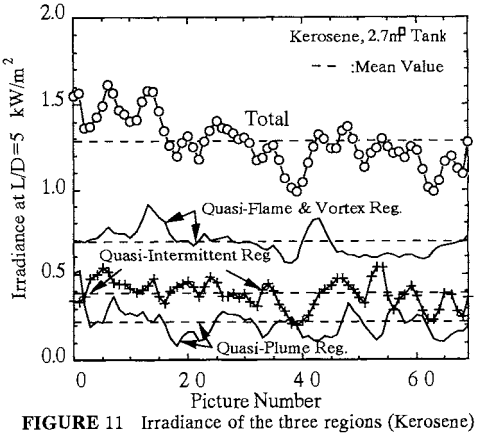

FIGURE 11 Irradiance of the three regions (Kerosene)

phy. Considering this, the ratios of each region to total irradiance are about 50% for quasi-flame and vortex, 30% for quasi-intermittent, and 20% for the quasi-plume region. In the heptane flame which has the largest irradiance and flame height, the irradiances of the quasi-intermittent region occasionally become greater than those of the quasi-flame and vortex regions, this occurred ten times in seven seconds. Such phenomena are rare for kerosene and crude oil flames, and accounts for the activity of the heptane flame in the quasi-intermittent region and the relatively high location of the highest radiance. Each region of irradiance has cyclic changes over about 0.1 - 0.3 seconds and the irradiance changes observed in the quasi-flame and vortex regions shift to the quasi-intermittent region and finally to the quasi-plume region. This supports the assumption that volumes of combustible gas mixture and air are successively formed near the tank and then move upward while burning, changing in shape and releasing radiation heat.

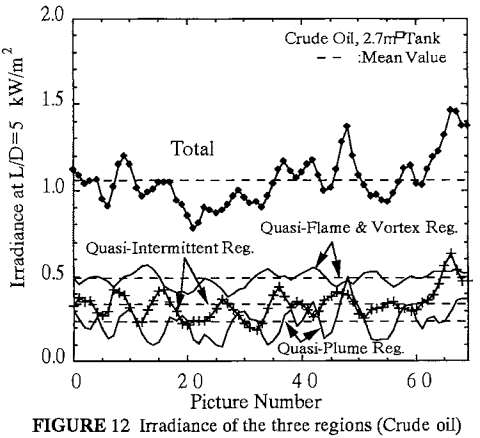

FIGURE 12 Irradiance of the three regions (Crude oil)

Irradiance of the quasi-flame region

With the boundary values of the coefficient of variation for stable flame region shown in Figures 7, 8, and 9, the quasi-flame and vortex regions can be divided into two, a quasi-flame or stable flame region and a quasi-vortex region. The hatched areas in Figures 7, 8, and 9 are the stable flame regions. The irradiances of each stable flame region are also extracted from thermographic data and is shown in Figure 13. The total irradiance and irradiance

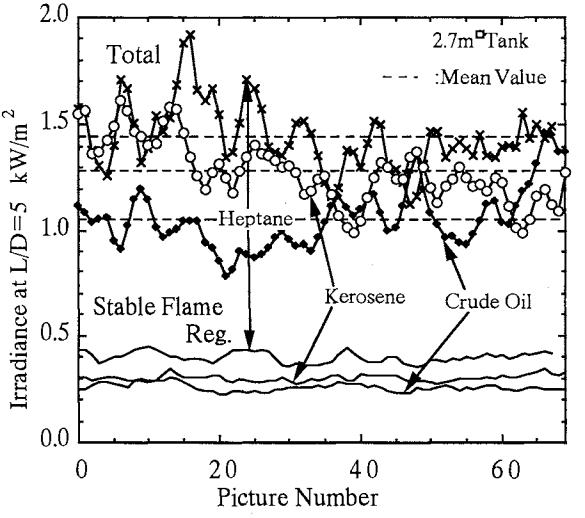

FIGURE 13 Irradiance of the stable flame region

of each stable flame region for the three fuels are shown together in Figure 13. The irradiance of each stable flame region is stable or appears horizontal lines despite the large changes in total irradiance. The ratio of irradiance of each stable flame region to the total irradiance are about 28% fro heptane, 24% for kerosene, and 25% for crude oil. From this result, we can conclude that different fuels have different flame structures and radiation characteristics, although the ratios of irradiance of each stable flame region to the total irradiance is around 25%. From a comparison of figures 10 to 12 and Figure 13, it is clear that almost all the fluctuations in the quasi-flame and quasi-vortex regions in Figures 10, 11, and 12 are mainly due to fluctuations in the quasi-vortex regions.

CONCLUSIONS

A new way of using thermography for radiative objects like pool flames is introduced and a statistical analysis using thermographic data to assess pool flame structure from a radiation point of view is considered. The discussion allows the following conclusions:

(1) A comparison with the results of other investigators show that the statistical analyses with thermographic data presented in this paper offers a useful and powerful approach to assess the flame structure of large pool fire flames.

(2) The contours of standard deviation, show regions with high values of standard deviation near the edges of flames. These regions appear to be closely related to vortex or flapping flames.

(3) The contours of the coefficient of variation, identify a stable flame region and the bottom of a quasi-plume region.

(4) The radiative properties of the stable flame, quasi-flame and vortex, quasi-intermittent, and quasi-plume regions are established.

ACKNOWLEDGMENTS

This research was assisted by a Grant in Aid for Science and Culture, Japan (No.04832001) and the Japanese Association of Fire Science and Engineering. I am grateful for these grants and to Nippon Avionics Co., LTD. for their help.

REFERENCES

1. Thomas, P.H.,"Some Experiments on Buoyant Diffusion Flames", Combustion and Flame, Vol.5, pp.359-367, 1961.

2. Akita, K. and Yumoto, T.,"Heat Transfer in Small Pools and Rates of Burning of Liquid Methanol", Tenth Symp. (Inter.) on Combustion, The combustion Institute, Pittsburgh, pp.943-948, 1965.

3. Yumoto, T.,"Heat Transfer from Flame to Fuel Surface in Large Pool Fires", Combustion and Flame, Vol.17, pp.108-110, 1971.

4. McCaffrey, B. J.,"Purely Buoyant Diffusion Flames : Some Experimental Results", Heptane Pool Fires", Fire Technology, Vol.24(1), pp.33-47, 1979.

5. Cetegen, B. M., Zukoski, E. E. and Kubota, T.,"Entrainment and Flame Geometry of Fire Plumes", NBS-GCR-82-402 (NBS,Washington, D.C.), pp.1-203, 1982.

6. Koseki. H. and Yumoto, T.,"Air Entrainment and Thermal Radiation from Heptane Pool Fires", Fire Technology, Vol.24(1), pp.33-47, 1988.

7. Ndubizu, C. C., Ramaker, D.E., Tatem, P.A., and Williams, F.W.,"A Model of Freely Burning Pool Fires", Combustion Science and Technology, Vol.31, pp.233-247, 1983.

8. Crocker, W. P. and Napier, D.H.,"Thermal Radiation Hazards of Liquid Pool Fires and Tank Fires", I.CHEM.E. Symposium Series No.97, pp.159-184, 1986.

9. Mudan, K. S.,"Thermal Radiation Hazards from Hydrocarbon Pool Fires", Prog. Energy and Combust. Sci., Vol.10, pp.59-80, 1984.

10. Koseki, H., and Hayasaka, H.,"Estimation of Thermal Balance in Heptane Pool Fire",Journal of Fire Sciences, Vol.7, pp.237-250, 1989.

11. Brötz, W., Schönbucher, A., Scheller, V. and Kettler A., "Electronically Produced Equidensities from Time Exposures and Instantaneous Photographs in the Investigation of Pool Flames", Combustion and Flame, Vol.37, pp.1-24, 1980.

12. Oka, Y. and Sugawa, S.,"Temperature Visualization of Extended Flame from Opening Using Infrared Image Processor", Fire Science and Technology, Vol.9(2), pp.15-22, 1989.

13. Hayasaka, H., Koseki, H., and Tashiro, Y.,"Radiation Measurements in Large-Scale Kerosene Pool Flames using High-Speed Thermography", Fire Technology, Vol.28(2), pp.110-122, 1992.

14. Hayasaka, H., Koseki, H., and Tashiro, Y.,"Radiation Measurements in Pool Flames using High-Speed Thermography", HTD-Vol. 203, ASME, pp.71-77, 1992.

15. Hägglund, B.,"The Heat Radiation from Petroleum Fires", Fire Research and Development News (Swedish), Vol.1, pp.18-24, 1977.

16. Bouhafid, A., Vantelon, J.P., Joulain, P. and Fernandez-Pello, A.C.,"On the Flame Structure at the Base of a Pool Fire", Twenty-Second Symp. (Inter.) on Combustion, The combustion Institute, Pittsburgh, pp.1291-1298, 1988.

17. Koseki. H. and Mulholland, G. W.,"The Effect of Diameter on the Burning of Crude Oil Pool Fires", Fire Technology, Vol.27(1), pp.54-65, 1991.